Liquid-crystalline elastomers

1999 J. Phys.: Condens. Matter 11 R239

(http://iopscience.iop.org/0953-8984/11/24/201)

J. Phys.: Condens. Matter **11** (1999) R239–R257. Printed in the UK PII: S0953-8984(99)97486-6

REVIEW ARTICLE

Liquid-crystalline elastomers

E M Terentjev

Cavendish Laboratory, University of Cambridge, Madingley Road, Cambridge CB3 0HE, UK

Received 22 January 1999

Abstract. Recent experimental and theoretical work shows that liquid-crystalline elastomers and gels have a highly mobile axis of anisotropy. Despite being nominally elastic solids, they also show features of fluids, such as the effect of soft elasticity. Work over the last few years is reviewed and some of the most important discoveries, as well as the outstanding problems in this field, are highlighted. We examine the unusual mechanical properties of nematic and smectic rubbers, their randomly disordered equilibrium textures, some aspects of dynamics and mechanical relaxation and the effect of uniform chiral piezoelectricity in amorphous polymer networks.

1. Introduction

Liquid-crystalline elastomers (LCE) and gels continue to fascinate scientists and engineers with the combination of physical properties that places them in a separate category from any other material. The core of this uniqueness lies in the orientational symmetry breaking and the resulting coupling of rubber elasticity and liquid-crystalline degrees of freedom. In ordinary elastic solids the deformations are created by relative movement of the same atoms (or molecules) that form the bonded low-symmetry lattice. Hence, when the deformation is small, the lattice symmetry is preserved and one obtains an ordinary elastic response (although often anisotropic); large deformations destroy the lattice integrity and simply break the material. In contrast, in elastomers and gels the macroscopic elastic response arises from the entropy change of polymer chains on relative movement of their cross-linked end points, which are relatively far apart. What happens to chain segments on a smaller length scale is a relatively independent matter. For instance, nematic order can be established within these chains and its director can rotate, in principle, independently of deformation of the cross-linking points. Such an internal degree of freedom within and coupled to the elastic body constitutes what is known as the Cosserat medium: the relative movement of cross-linking points provides elastic strains and forces, while the director rotation causes local torques and couple stresses. However, the liquid-crystalline elastomer is even richer than notional Cosserat solids because (again due to the entropic nature of long polymer chains connecting the cross-linking points) rubbers are capable of very large shear deformations (being at the same time essentially incompressible). Hence, one expects a variety of unique physical properties, especially in the region of large deformations. Indeed, some such properties have been reported in recent years.

It is important to realize that a unique physical system, such as liquid-crystalline elastomers and gels, should be looked upon from the point of view of equally unique applications. Because of their slow dynamics and the high fields required to overcome the elastic resistance, LCE are poor for electro-optical display devices, which is one of the main thrusts in conventional liquid crystals. Because of their chemical complexity, they are not optimal for shoe soles and

tennis balls (although for 'high-tech' rubber tyres this is perhaps an open question). What LCE seem to be made for is the manipulation of the axis of optical birefringence by mechanical means. Unusual non-symmetric elasticity, with very low shear modulus and high impedance, is another characteristic physical property still waiting for an appropriate application system. The third prospective area is rubbers with piezoelectric and non-linear optic properties which, again in contrast to traditional crystalline and ceramic materials, allow large deformations and manipulation of polarization by mechanical means.

After the concept of nematic elastomers was put forward by de Gennes in 1975 [1] and the first side-chain liquid-crystalline polymer was cross-linked into elastomer by Finkelmann *et al* in 1981 [2], the initial research has been mainly focusing on synthetic and characterization work. The reviews [3–6] give a comprehensive picture of that period. In recent years the emphasis has been gradually shifting towards studies of new physical properties and the geography of research into liquid-crystalline elastomers has been significantly broadened.

1.1. Synthesis

For many years the prevailing type of LCE-forming materials were the side-chain liquid-crystalline polymers. Since the early work of Ringsdorf and Finkelmann, polyacrylate backbones with a number of mesogenic pendants have been used by different groups [7–9] to produce a variety of LCE. However, it has been quickly recognized that polyacrylate-based polymer chains have certain practical disadvantages, in particular the high glass transition temperature $T_g \geqslant 50\,^{\circ}$C and low backbone anisotropy. Side-chain liquid-crystalline polymers based on siloxane backbones have shown more dramatic mechanical properties due to a much higher chain anisotropy and are conveniently liquid crystalline at room temperature (with $T_g \leqslant 5\,^{\circ}$C). Methods of cross-linking have varied from chemical, using copolymerization with a small proportion of reactive groups on a chain and adding bi- or tri-functional cross-linking agents [10, 11], to radiation processes using UV light with photoinitiators [12] or gamma radiation [13].

Much less synthetic work has been done on networks of main-chain mesogenic polymers, apart from the long history of mesogenic epoxy resins prepared over the years by Carfagna *et al* [14] and Ober *et al* [4]. In the last 2–3 years, however, there has been a noticeable surge of activity in this area. An interesting group of rigid-rod polymers, somewhat echoing the activity in stiff-chain Kevlar-type fibres [15], but showing remarkable liquid-crystalline properties in a swollen state, were prepared by Zhao *et al* [16] (polyisocyanate chains were cross-linked into networks by hydrosilation reaction). The Cornell group has produced lightly cross-linked (i.e. rubbery without swelling) nematic and smectic elastomers based on the rod-like mesogenic monomers connected via flexible spacers [17, 18]. Finkelmann and co-workers have prepared another group of nematic main-chain elastomers based on semi-flexible polyether chains [19]. In all of these new reports the synthetic work was accompanied by important physical experiments, characterizing the stress–strain behaviour and the stress-induced alignment. One expects, and indeed finds, dramatic elastic effects (in the range of strains up to 3–400%) due to the high chain anisotropy of main-chain mesogenic polymers.

Another interesting lyotropic LCE system (showing the mesogenic behaviour in response to changes in solvent concentration, water in this case) has been prepared in Freiburg [20]. The material is based on the lamellar phase of side-chain polysurfactant. This work explores a concept of permanently tethering the layers via cross-linking across them, either through the hydrophobic polymer backbone or through hydrophilic side-chains.

1.2. Physical properties

One of the main difficulties preventing a widespread effort in experimental studies of LCE is their sparse availability. Because a complicated synthesis is required, the cross-linked (or cross-linkable) liquid-crystalline polymers are not available commercially and are only produced in the research laboratories mentioned in the previous section. Nevertheless, the last few years have seen a substantial increase in experimental research. One factor contributing to this increase is the growing ability of synthetic groups to perform sophisticated physical experiments: many of the remarkable physical properties have been discovered in the laboratories where the materials have been prepared (see, for instance, [21–23] described below). Another factor is the increasing ease of preparing basic LCE systems, which allows some more traditional physics research groups to enter the field; see, for example, [24, 25]. One way or another, many characteristic physical properties of LCE have been studied over the years. Below, we shall examine some of the most important recent discoveries related to structure and mechanical response, electric field and polarization properties, and dynamical effects.

In the next section we shall recall the main features of Cosserat-like nematic rubber elasticity, using the limit of continuum linear theory to illustrate the similarities to and differences from the conventional symmetric elasticity of crystalline solids. This level of approximation, assuming small deformations, is not very characteristic of a rubber capable of undergoing very large strains. However, it serves the purpose of illustration and, besides, is fully applicable to a number of physical effects naturally involving small deformations, e.g. acoustic waves, or thermal fluctuations.

The following sections describe recent advances in several key areas of physical properties of LCE. The theoretically predicted effect of soft elasticity, a remarkable phenomenon when there is no rubber-elastic energy in response to certain sets of strains, have been confirmed by several experimental findings. The role of quenched random disorder in forming the equilibrium polydomain textures and in controlling the slow dynamics of deformations in LCE has become clearer in the last few years, making an attractive parallel with a number of glass systems. The additional one-dimensional translational symmetry breaking in smectic or lamellar elastomers and gels makes them equally puzzling and provocative physical systems, with a characteristic two-dimensional entropic rubber elasticity within the layers and a very rigid solid-like response to deformations along the layer normal. Finally, much progress has been made recently in theoretical and experimental studies of piezoelectric effects in chiral LCE and we shall review the main points of principle in this area.

2. Nematic rubber elasticity

Rubber-elastic response to deformations of a polymer network stems from the entropy change when the number of conformations allowed for the chains is reduced on stretching their end-to-end distance terminated by network cross-links. Within the simplest affine deformation approach one regards the change in each chain end-to-end vector $\boldsymbol{R}$ as $\boldsymbol{R}' = \underline{\underline{\boldsymbol{\lambda}}} \cdot \boldsymbol{R}$, when a deformation characterized by a Cauchy strain tensor λ_{ij} is applied to the whole sample. Assuming that the chain connecting the two cross-links is long enough, the Gaussian approximation for the number of its conformations gives for the free energy (per chain)

$$F_{ch} = -kT \ln W(\boldsymbol{R}') \simeq kT \frac{1}{a^2 N} (\underline{\underline{\boldsymbol{\lambda}}}^{\mathrm{T}} \cdot \underline{\underline{\boldsymbol{\lambda}}})_{ij} R_i R_j$$

where a is the step length of the chain random walk and N the number of such steps. In order to find the total free energy of all chains affinely deforming in the network, one needs to add the

contributions $F_{ch}(R)$ with statistical weighting to find a chain with a given initial end-to-end distance $\boldsymbol{R}$ in the system. This procedure, called quenched averaging, produces the average $\langle R_i R_j \rangle \simeq \frac{1}{3}a^2 N \delta_{ij}$ in the expression for F_{ch}. The resulting rubber-elastic free energy (per unit volume) is $F_{el} = \frac{1}{2}n_c kT(\underline{\underline{\lambda}}^{\mathrm{T}} : \underline{\underline{\lambda}})$, with n_c a number of chains per unit volume of the network. This is a remarkably robust expression, with many seemingly relevant effects, such as the fluctuation of cross-linking points, only contributing a small quantitative change in the prefactor. The value of the rubber modulus is found on expanding the Cauchy strain tensor in small deformations, say, $\lambda_{zz} = 1+\varepsilon$, and obtaining $F_{el} \simeq \frac{1}{2}\mu\varepsilon^2$ with $\mu = n_c kT$. This modulus, having its origin in the entropic effect of reduction of conformational freedom on polymer chain deformation, is usually so much smaller than the bulk modulus (determined by the enthalpy of compressing the dense polymer liquid) that the rubber is considered as deforming at constant volume. This constraint leads to the familiar expression $F_{el} = \frac{1}{2}n_c kT(\lambda^2 + 2/\lambda)$ where one has assumed that the imposed extension $\lambda_{zz} = \lambda$ is accompanied by symmetric contraction in both transverse directions, $\lambda_{xx} = \lambda_{yy} = 1/\sqrt{\lambda}$, due to the incompressibility.

When the chains forming the rubbery network are liquid crystalline, their end-to-end distance distribution becomes anisotropic. In the case of a simple uniaxial nematic one obtains $\langle R_\parallel R_\parallel \rangle = \frac{1}{3}\ell_\parallel L$ and $\langle R_\perp R_\perp \rangle = \frac{1}{3}\ell_\perp L$, with $L = aN$ the chain contour length and $\ell_\parallel/\ell_\perp$ the ratio of average chain step lengths along and perpendicular to the nematic director. In the isotropic phase one recovers $\ell_\parallel = \ell_\perp = a$. The uniaxial anisotropy of polymer chains has a principal axis along the nematic director $\boldsymbol{n}$, with a prolate ($\ell_\parallel/\ell_\perp > 1$) or oblate ($\ell_\parallel/\ell_\perp < 1$) ellipsoidal conformation of the polymer backbone. The ability of this principal axis to rotate independently under the influence of network strains makes the rubber-elastic response non-symmetric (see the review [5] for details of the molecular theory of nematic rubber elasticity), so we have

$$F_{el} = \frac{1}{2}\mu\,\mathrm{Tr}(\underline{\underline{\lambda}}^{\mathrm{T}} \cdot \underline{\underline{\ell}}_\theta^{-1} \cdot \underline{\underline{\lambda}} \cdot \underline{\underline{\ell}}_0) + \frac{1}{2}\tilde{B}\big(\mathrm{Det}[\underline{\underline{\lambda}}] - 1\big)^2 \tag{1}$$

with $\underline{\underline{\ell}}$ the uniaxial matrices of chain step lengths before (0) and after the director has rotated by an angle θ:

$$\ell_{ij} = \ell_\perp \delta_{ij} + [\ell_\parallel - \ell_\perp] n_i n_j .$$

The last term, the additional bulk-modulus contribution independent of the configurational entropy of polymer chains, is determined by molecular forces resisting the compression of a molecular liquid, $\tilde{B} \sim 10^{10}$–10^{11} J m^{-3}, much greater than the typical value of the rubber modulus $\mu \sim 10^5$ J m^{-3}. This large energy penalty constrains the value of the strain determinant, $\mathrm{Det}[\underline{\underline{\lambda}}] \approx 1$ (which, in other words, means that the material is physically incompressible).

Note that the Cauchy strain tensor $\underline{\underline{\lambda}}$ no longer enters the elastic energy in the symmetric combination $\underline{\underline{\lambda}}^{\mathrm{T}} \cdot \underline{\underline{\lambda}}$, but is now 'sandwiched' between the matrices $\underline{\underline{\ell}}$ with different principal axes. This means that antisymmetric components of strain will now have a non-trivial physical effect, in contrast to the case for isotropic rubbers and, more crucially, to the case for elastic solids with uniaxial anisotropy. There, the anisotropy axis is immobile and the response is anisotropic but symmetric in stress and strain. The uniqueness of nematic rubbers stems from the competing microscopic interactions and the difference in characteristic length scales: the uniaxial anisotropy is established on a small (monomer) scale of the nematic coherence length, while the strains are defined (and the elastic response is arising) on a much greater length scale of the polymer chain end-to-end distance (see figure 1).

The similarities to, and areas of contrast with the conventional uniaxial elasticity are more apparent on the level of linear continuum description, when only small deformations and small director rotations are considered. Introducing the deformation tensor v_{ij} as the gradient of the

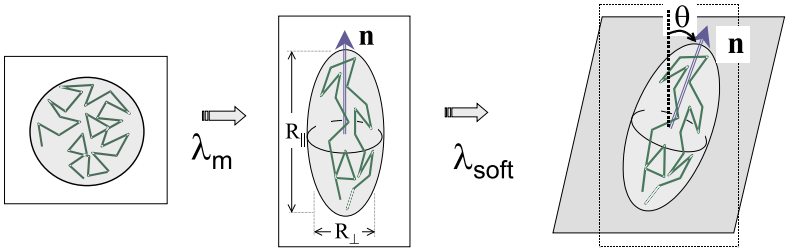

Figure 1. The relation between the equilibrium chain shape and deformations in LCE. When the network of initially isotropic chains, forming a spherical gyration shape (a), is brought into the uniform nematic phase (b), a corresponding spontaneous deformation of the sample occurs in proportion to the backbone anisotropy, $\lambda_m \approx (\ell_\parallel/\ell_\perp)^{-1/3}$. An example of soft deformation (c), when rotating anisotropic chains, can affinely accommodate all strains (a combination of compression along the initial director, extension across it and a shear in the plane of the director rotation), not causing any entropic rubber-elastic response.

local displacement vector $\boldsymbol{v}$ ($\mathsf{v}_{ij} = \nabla_i v_j$, with the Cauchy strain $\lambda_{ij} = \delta_{ij} + \mathsf{v}_{ij}$ taken to be incompressible, with $\mathrm{Det}[\underline{\underline{\boldsymbol{\lambda}}}] = 1$), one obtains

$$F = \frac{1}{2}\mu_0(\boldsymbol{n}\cdot\tilde{\underline{\underline{\varepsilon}}}\cdot\boldsymbol{n})^2 + \frac{1}{2}\mu_1[\boldsymbol{n}\times\tilde{\underline{\underline{\varepsilon}}}\times\boldsymbol{n}]^2 + \frac{1}{2}\mu_2(\boldsymbol{n}\cdot\tilde{\underline{\underline{\varepsilon}}}\times\boldsymbol{n})^2 + \frac{1}{2}D_1[(\boldsymbol{\Omega}-\boldsymbol{\omega})\times\boldsymbol{n}]^2 + \frac{1}{2}D_2\boldsymbol{n}\cdot\tilde{\underline{\underline{\varepsilon}}}\cdot[(\boldsymbol{\Omega}-\boldsymbol{\omega})\times\boldsymbol{n}] + \frac{1}{2}K(\nabla\boldsymbol{n})^2 \tag{2}$$

where $\tilde{\underline{\underline{\varepsilon}}}$ is the symmetric traceless part of the deformation tensor, $\frac{1}{2}(\underline{\underline{\mathsf{v}}}+\underline{\underline{\mathsf{v}}}^{\mathrm{T}}) - \frac{1}{3}\underline{\underline{\boldsymbol{\delta}}}\,\mathrm{div}\,\boldsymbol{v}$, the only relevant variable in the conventional linear elastic theory†. Two vectors, $\boldsymbol{\Omega}$ and $\boldsymbol{\omega}$, describe the rotational contributions of deformation ($\boldsymbol{\Omega} = \frac{1}{2}\,\mathrm{curl}\,\boldsymbol{v}$, the antisymmetric part of $\underline{\underline{\mathsf{v}}}$) and the nematic director ($\boldsymbol{\omega} = [\boldsymbol{n}\times\delta\boldsymbol{n}]$). The unit vector $\boldsymbol{n}$ in (2) represents the axis of uniaxial anisotropy before deformation and should be regarded as fixed at this level of approximation, except in the traditional nematic Frank-elasticity contribution, the last term in the continuum free-energy density (2), schematically presented in the one-constant approximation. Clearly, only the uniform *relative rotation* of the nematic and rubber-elastic subsystems contributes to the free energy (2) via the coupling terms D_1 and D_2, first written down phenomenologically by de Gennes [26]. Applying a particular molecular model, equation (1) [5], one finds the values of the relevant constants:

$$\mu_0 = \mu_1 = 2n_ck_BT \qquad \mu_2 = n_ck_BT\left(\frac{\ell_\parallel^2+\ell_\perp^2}{\ell_\parallel\ell_\perp}\right)^2$$
$$D_1 = n_ck_BT\left(\frac{\ell_\parallel^2-\ell_\perp^2}{\ell_\parallel\ell_\perp}\right)^2 \qquad D_2 = n_ck_BT\,\frac{\ell_\parallel^2-\ell_\perp^2}{\ell_\perp^2}. \tag{3}$$

Appropriately, the relative-rotation coupling constants must vanish in the isotropic phase, at $\ell_\parallel = \ell_\perp$. Many molecular models of nematic polymer chains relate the average backbone anisotropy $(\ell_\parallel/\ell_\perp - 1)$ to the local nematic order parameter Q, defined as the thermodynamic average of mesogenic monomer long axes $\langle\frac{3}{2}(\boldsymbol{u}\cdot\boldsymbol{n})^2 - \frac{1}{2}\rangle$. One then finds that D_1 must scale as μQ^2 because the penalty on relative rotation $\sim(\boldsymbol{\Omega}-\boldsymbol{\omega})^2$ cannot depend on the sign of Q, i.e. on whether the polymer chains are prolate or oblate. In contrast, D_2 must scale as μQ

† The symbolic second-rank tensor $[\boldsymbol{n}\times\underline{\underline{\varepsilon}}\times\boldsymbol{n}]$ is shorthand for the matrix product $A_{\alpha\beta} = \epsilon_{\alpha jk}n_j\varepsilon_{kl}n_m\epsilon_{ml\beta}$ (symmetric, $A_{\alpha\beta} = A_{\beta\alpha}$). Similarly, the symbolic vector $(\boldsymbol{n}\cdot\underline{\underline{\varepsilon}}\times\boldsymbol{n})$ is shorthand for the matrix product $n_k\varepsilon_{kl}n_m\epsilon_{ml\alpha}$.

because the signs of the director rotations induced by symmetric shear $\underline{\underline{\varepsilon}}$ are different in prolate and oblate elastomers:

$$D_1 \propto (\ell_\parallel - \ell_\perp)^2 \sim Q^2 \qquad \text{and} \qquad D_2 \propto (\ell_\parallel - \ell_\perp) \sim Q.$$

Two main consequences of the coupling between the elastic modes of the polymer network and the rotational modes of the nematic director are the reduction of the effective elastic response and the penalty on the director fluctuations. The first effect has been given the name 'soft elasticity' and is the result of integrating out (minimizing over) the director fluctuations $\delta\boldsymbol{n}$ in the expression for F_{el} in (2). In some cases this may even result in the total elimination of elastic response, e.g. the renormalized shear modulus $\tilde{\mu}_2 \to 0$, and reflects the ability of anisotropic polymer chains to rotate their long axis to accommodate some imposed elastic deformations without changing their shape. If one instead chooses to focus on the director modes in a nematic elastomer with a fixed (constrained) shape, the coupling terms D_1 and D_2 provide a large energy penalty for uniform director rotations $\delta\boldsymbol{n}$ (with respect to the elastically constrained network). This penalty, which appears as a mass term in the expression for the mean square director fluctuation

$$\langle|\delta\boldsymbol{n}_q|^2\rangle \simeq \frac{k_B T}{V(Kq^2 + \tilde{D})}$$

with K the Frank constant, results in the suppression of fluctuations and the related scattering of light from a nematic elastomer. In contrast to optically turbid ordinary liquid nematics, where light is scattered by long-wavelength director fluctuations, aligned monodomain nematic rubber is totally transparent. However, when the elastic deformations in the network are not constrained and are free to relax, there are certain combinations of polarization and wave vectors of director fluctuations (corresponding to the soft-deformation modes) for which the 'effective mass' $\tilde{D}$ vanishes and the fluctuation spectrum should appear as in ordinary liquid nematics [27].

3. Soft elasticity and stripe domains

For several years it was understood that if a sample of monodomain, uniformly aligned nematic elastomer (which usually implies that it has been cross-linked in the aligned nematic phase [8, 10]) is stretched along the axis perpendicular to the nematic director $\hat{\boldsymbol{n}}_0$, the director will switch and point along the axis of uniaxial extension. The early theory (ignoring the effect of soft elasticity) [28] has predicted and the experiment on polyacrylate LCE [29] reported that this switching occurs in an abrupt discontinuous fashion when the natural long dimension of anisotropic polymer chains can fit into the new shape of the sample, much extended in the perpendicular direction. However, in 1995, the same experiment performed on a polysiloxane LCE [21] has shown an unexpected stripe domain pattern. Further investigation has proven that the nematic director rotates continuously from $\hat{\boldsymbol{n}}_0$ towards the new perpendicular axis, over a substantial range of deformations, but the direction of this rotation alternates in semi-regular stripes several microns in width oriented along the stretching direction; see figure 2(a). Later, the same textures were observed by other groups and for different materials, including polyacrylates [11, 30], although there also is an unambiguous report of the single-director switching mode [31].

Theoretical description of stripe domains [32] has been successful in describing diverse and complicated physical effects of the Cosserat-like elastic medium at large deformations in a non-uniform texture. One of the results gives the director angle variation with strain:

$$\theta(\lambda) = \pm \arcsin\left[\frac{\ell_\parallel}{\ell_\parallel - \ell_\perp}\left(1 - \frac{\lambda_c^2}{\lambda^2}\right)\right]^{1/2} \tag{4}$$

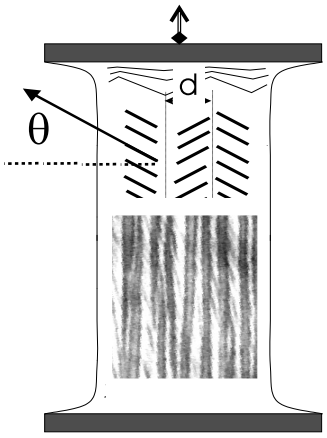

(a)

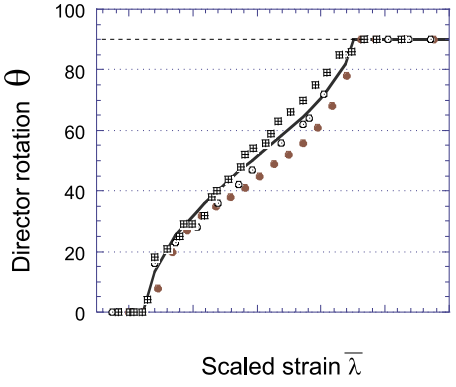

(b)

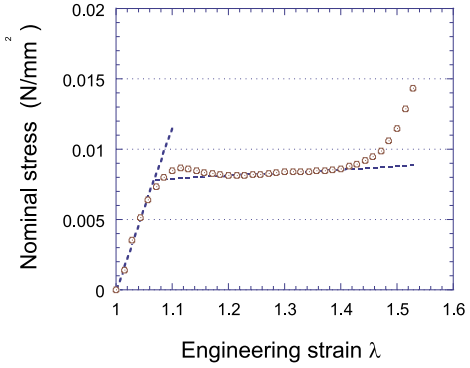

(c)

Figure 2. Stripe domains in nematic LCE. (a) A schematic picture of alternating domains with $\pm\theta$ on stretching the sample perpendicular to the nematic director $\boldsymbol{n}$; the inset shows a microscopic image of stripes between crossed polars. (b) The director rotation angle $\theta(\lambda)$ in each domain—the theoretical curve, equation (4), and several different experiments collapsed on it by rescaling of variables. (c) An associated stress–strain curve showing the soft-elasticity plateau in a sample of polysiloxane LCE with flexible tri-functional cross-links. Note a small hump at the beginning of the soft region, which is due to an extremely slow stress relaxation at the moment when the stripe domains are being formed by negotiating between local shears and mechanical constraints.

with only one free parameter, the threshold strain λ_c. The backbone chain anisotropy $\ell_\parallel/\ell_\perp$, which enters the theory, is an independent experimentally accessible quantity related, e.g. to the spontaneous shape change of LCE on heating it into the isotropic phase, $\lambda_m \approx (\ell_\parallel/\ell_\perp)^{1/3}$ in figure 1. This allowed the data for the director angle, obtained in different experiments on many different materials, to be collapsed onto the same master curve (figure 2(b)), spanning the whole range of non-linear deformations. More importantly, the good correspondence between the theory and experiment became the first unambiguous proof of the soft-deformation regime.

The physical reason for the stretched LCE breaking into stripe domains with opposite director rotations, $\pm\theta(\lambda)$, becomes clear when one recalls the idea of soft elasticity [27, 33]. The polymer chains forming the network are anisotropic, in most cases having the average shape of a uniaxial prolate ellipsoid; see figure 1. If the assumption of affine deformation is made, the strain applied to the whole sample is locally applied to all network strands. The origin of (entropic) rubber elasticity is the corresponding change of shape of the chains, away from their equilibrium shape frozen at network formation, which results in the reduction in entropy and rise in the elastic free energy. However, the nematic (e.g. prolate anisotropic) chains may find another way of accommodating the deformation: if the sample is stretched perpendicular to the director $\boldsymbol{n}$ (the long axis of the chain gyration volume), the chains may rotate their *undeformed* ellipsoidal shapes—thus providing an extension, but necessarily in combination with simple shear—and keep their entropy constant and elastic free energy zero! This, of course, is unique to nematic elastomers: isotropic chains (with spherical shape) have to deform to accommodate any deformation. Mathematically, Olmsted [27] has shown that there is a continuous set of such soft deformations, which by appropriately combining strains and director rotations can make the elastic response vanish, expressed by the matrix product

$$\underline{\underline{\boldsymbol{\lambda}}} = \underline{\underline{\boldsymbol{\ell}}}_\theta^{1/2} \cdot \underline{\underline{\mathbf{V}}} \cdot \underline{\underline{\boldsymbol{\ell}}}_0^{-1/2}$$

where the $\underline{\underline{\boldsymbol{\ell}}}$ are the step-length tensors before and after the director rotation and $\underline{\underline{\mathbf{V}}}$ is an arbitrary unitary matrix. The physical explanation of stripe domains is now clear: the stretched LCE attempts to follow the soft-deformation route to reduce its elastic energy, but this requires a shear deformation which is prohibited by rigid clamps on two opposite ends of the sample; figure 2(a). The solution is to break into small stripes, each with a completely soft deformation (and a corresponding shear) but with the sign of director rotation (and thus also the shear) alternating between the stripes. Then there is no global shear and the system can lower its elastic energy in the bulk, although it now has to pay the penalty for domain walls and for the non-uniform region of deformation near the clamps. The balance of gains and losses determines the domain size.

The argument above seems to provide a reason for the threshold strain λ_c, which is necessary to overcome the barrier for creating domain walls between the 'soft' stripes. However, it turns out that the numbers do not match. The threshold provided by domain walls alone should be very small (the strain being a fraction of one per cent), whereas most experiments have reported $\lambda_c \sim 1.1$ or more. This caused theoreticians to develop a whole new concept of what is now called 'semi-softness' of LCE. The idea is that, due to several different microscopic mechanisms [34], a small addition to the classical nematic rubber-elastic free energy is breaking the symmetry required for the soft deformations:

$$F \simeq \frac{1}{2}\mu \left[\mathrm{Tr}(\underline{\underline{\boldsymbol{\lambda}}}^{\mathrm{T}} \cdot \underline{\underline{\boldsymbol{\ell}}}_\theta^{-1} \cdot \underline{\underline{\boldsymbol{\lambda}}} \cdot \underline{\underline{\boldsymbol{\ell}}}_0) + \alpha(\delta\boldsymbol{n} + \boldsymbol{n} \cdot \underline{\underline{\boldsymbol{\lambda}}} \times \delta\boldsymbol{n})^2 \right] \tag{5}$$

(usually $\alpha \ll 1$). The soft-elastic pathways are still representing the low-energy deformations, but the small penalty $\sim\alpha\mu$ provides the threshold for stripe domain formation and also makes the slope of the stress–strain soft-elastic plateau small but non-zero; see figure 2(c).

Regardless of the small 'complications' of semi-soft corrections, the main advance in identifying the whole class of special low-energy soft deformations in LCE and proving their existence by direct experiment is worth noting.

4. Random disorder in nematic networks

It was recognized long ago that, if no special precautions are taken to preserve the monodomain director alignment in the network, the LCE always form with a highly disordered director texture. Although this seems similar to the case for liquid-crystalline polymers and even to that for low-molar-mass liquid crystals, the major difference is that this disordered director texture represents a thermodynamic equilibrium in elastomers. If such a material is made uniformly aligned by application of an external field or mechanical stretching, it always returns back to its disordered state after the external aligning influence is removed.

The concept of quenched sources of random orientational disorder, represented in LCE by network cross-links imposing a local field on the director in their immediate vicinity, has been put forward to account for the resulting equilibrium 'polydomain' state [35]. Polydomain is put in quotes because, similarly to the case for the analogous effect in random-anisotropy spin glasses, there are no uniform domains with sharp boundaries. The average distance between disclinations in a typical Schlieren texture represents the size of different correlated regions within which the nematic director $\boldsymbol{n}$ is more or less aligned, and is a characteristic length scale of the texture. The basic scaling observation, that at long scales the static random distortions dominate over the dynamic thermal fluctuations, has been verified by rigorous theoretical analysis and experimental studies of correlations and susceptibilities in a wide variety of systems; see, for instance, [36]. The critical slowing down of all relaxation processes in systems with a random, glass-like order is also a well-established universal phenomenon [37,38]. When a polymer network is cross-linked in the isotropic state and then brought down in temperature into the nematic phase, the misoriented anisotropic cross-links act as local quenched sources of disorder for the nematic director field, in full analogy to magnetic impurities in spin glasses. The resulting equilibrium texture is characterized by rapidly decaying correlation in the director orientation, crudely

$$\langle \cos\theta(r)\cos\theta(0)\rangle \sim \exp[-r/\xi]$$

imposing a length scale ξ that is often called the 'domain size'. It is most important to emphasize that this length scale is macroscopic, although the average distance between cross-linking points could be measured as a few nanometres. The domain size ξ is determined by the balance between two opposite effects, the coarse-grained continuum random field of cross-links, parametrized by its intensity Γ depending to the cross-linking density, and the aligning effect of Frank elasticity, with the constant K determined by the local nematic order Q; very approximately $\xi \simeq K^2/\Gamma$ and may reach several microns in magnitude [39].

The local coupling constant of the nematic director field and the anisotropic (e.g. rigid-rod [34]) cross-link is not an easy parameter to evaluate from molecular models. The authors of [34] have estimated such a constant as $g \sim (k_B T/N)\Delta Q$, where N is the number of monomers on an average network strand, Δ a measure of the geometric anisotropy (e.g. the aspect ratio of a rod-like cross-linking molecule) and Q the local nematic order parameter of the matrix. The quenched averaging of the random orientational field from all such local sources produces an estimate for the coarse-grained intensity:

$$\Gamma \simeq n_c g^2 \propto n_c^3 Q^2$$

very crudely.

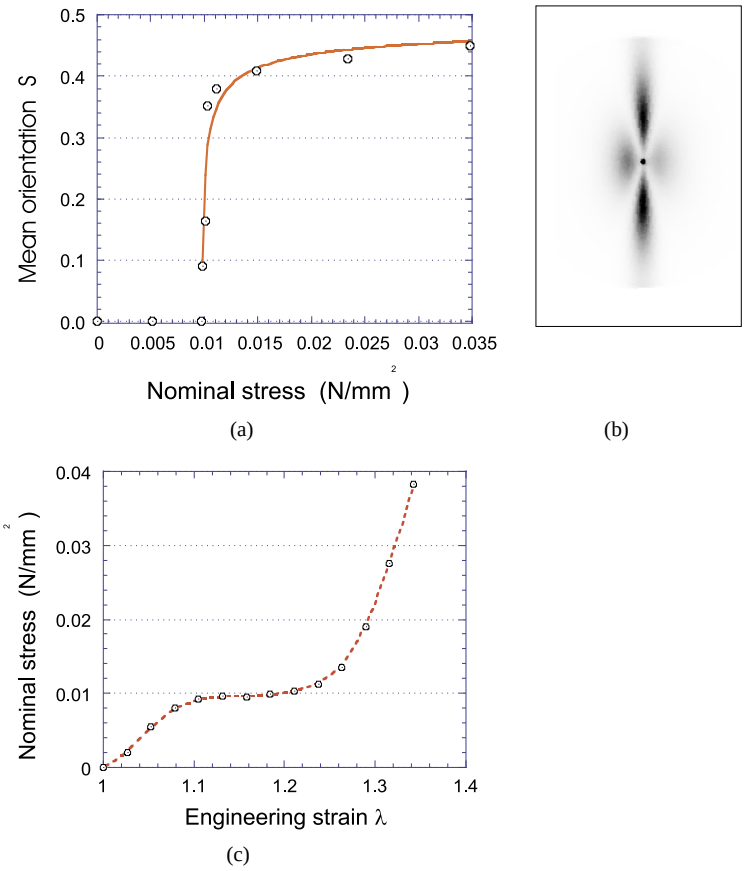

Figure 3. Polydomain–monodomain transition in LCE. (a) The mean orientation parameter $S(\sigma)$, equation (6), with experimental data on polysiloxane LCE [41]. (b) The light scattering image with four peaks produced by the optical contrast between misoriented 'domains' viewed through crossed polars. The angular position of the peaks corresponds to the correlation length $\xi \sim 2\,\mu$m, slightly anisotropic in the direction of stretching. (c) The stress–strain curve for the transition in polysiloxane side-chain LCE, which shows the soft plateau in the region of transition; the plateau stress value is the critical stress σ_c in panel (a).

If one applied a strong external field to a randomly disordered system, e.g. a spin glass, it would form long-range-order correlations and align along the field direction. The corresponding polydomain–monodomain transition in LCE, induced by uniaxial stretching, has been known of for a long time. Recent theoretical work [40] predicted a threshold stress $\sigma_c \sim \mu Q$ due to energy barriers provided by elastic incompatibility between different domains. An important observable quantity is the parameter of mean director orientation between the domains, $S = \langle \frac{3}{2}\cos^2\theta - \frac{1}{2}\rangle$, where the angle θ measures the deviation of a local director $\boldsymbol{n}(\boldsymbol{r})$ (the principal axis of the local nematic order, the magnitude of which is measured by Q) and, for instance, the direction of the imposed field. This mean orientation parameter shows an unusual exponential variation above σ_c, approximately given by

$$S \simeq Q \exp\left[-\frac{1}{2}\frac{K^{3/2}}{\xi(\sigma-\sigma_c)^{1/2}}\right] \tag{6}$$

with a small jump at the threshold. At a high stress, much larger than the threshold, the

mean orientation parameter follows the asymptotic behaviour $S \approx Q \exp[-K^2/kT\xi\sigma]$ (at $\sigma \gg \sigma_c$) and approaches its maximal value, equal to the local nematic order parameter Q. More specific experiments have focused on this transition. It appears that the threshold stress is very low in polyacrylate side-chain elastomers [13] with small backbone chain anisotropy and is larger in polysiloxanes [41] and even more so in highly anisotropic main-chain LCE [17]. It also appears that, as the theory predicted, the transition proceeds via the reorientation of different domains rather than the growth of correctly aligned domains. As we know, the director rotation leads to a change in sample shape if the system is allowed to follow the low-energy soft-deformation pathway and, therefore, it is not surprising to see the stress plateau during the polydomain–monodomain transition; see figure 3(c). One should add that such a flat, almost exactly soft plateau is not always seen in experiment; frequently the semi-soft slope of $\sigma(\lambda)$ in the transition region is substantial. The reason for this is thought to be related to the effect of domain wall localization [40] under strain, when the initially very broad non-uniform regions of director variation become narrow (similarly to the case for the walls between stripe domains discussed above) to allow the greater volume of the material to undergo soft deformation. This localization may be strongly resisted in different materials depending on the rigidity of cross-links and other possible impurities.

The concept of randomly quenched disorder and the analogy with spin glasses makes the polydomain LCE an interesting physical system on its own. We shall see below that it has a strong effect on low-frequency dynamic properties, causing a particularly slow relaxation of mechanical stress.

5. Smectic elastomers

Smectic elastomers and gels, or permanently cross-linked networks of polymers that spontaneously form smectic or lamellar phases, are just as frequently found as the nematic ones. There are a great variety of possible phases, combining the one-dimensional layered order with various degrees of structure and alignment of mesogenic groups. We shall only consider the simplest smectic order, appropriately called the 'smectic-A' or lamellar L_α phase, where the uniaxial molecular anisotropy is coaxial with the layer normal. In other words, the nematic director (which is the principal axis of optical birefringence) is locked perpendicular to the smectic layers. Accordingly, if the deformation of layers occurs in such a way that a local tilt is produced, it can be described either by the gradients of the scalar layer displacement field $u(\boldsymbol{r})$ or via the director rotations $\delta\boldsymbol{n}$. For instance, when the undistorted layer normal (and the nematic director $\boldsymbol{n}$) is along $\boldsymbol{z}$ one obtains $\delta\boldsymbol{n}_x = -\partial u/\partial x;\ \delta\boldsymbol{n}_y = -\partial u/\partial y$. A direct result of the spontaneous layered structure is the penalty on layer compression. Again, if the layer normal is chosen along the z-axis, the compression $\partial u/\partial z$ is the measure of the local deviation of the layer spacing from its equilibrium value d_0. This elastic penalty has a consequence of prohibiting the bend and twist deformations of the nematic director which acts as the local layer normal. These considerations lead to the well-known expression for the elastic energy density of a smectic phase, written in the form where the deformation is parametrized by the local layer displacement field $u(\boldsymbol{r})$ and consisting of just two terms: the layer compression penalty and the splay deformation contribution $K_1(\operatorname{div}\boldsymbol{n})^2$:

$$F_{sm} = \frac{1}{2}B\left(\frac{\partial u}{\partial z}\right)^2 + \frac{1}{2}K_1\left[\left(\frac{\partial^2 u}{\partial x^2}\right)^2 + \left(\frac{\partial^2 u}{\partial y^2}\right)^2\right] \tag{7}$$

where the undistorted layer normal $\boldsymbol{n}$ is taken along $\boldsymbol{z}$. By dimensional arguments, one always expects to find the ratio $\sqrt{K/B} \sim d_0$, the smectic-layer spacing.

When the smectic order is formed in an elastomer, one needs to examine the coupling between layer deformations $u(\boldsymbol{r})$ and those of the rubbery network, the cross-linking points of which are displaced by the vector $\boldsymbol{v}(\boldsymbol{r})$. From the continuum point of view, the local symmetry of smectic-A phase is exactly the same as that of a nematic (the additional translational symmetry breaking leading to the compression penalty and the above constraints on possible non-uniform deformations). Accordingly, the coupling terms fall into three categories. One is due to the local point symmetry, equivalent to the nematic uniaxial order, and leads to the two relative-rotation terms D_1 and D_2 that appear in the corresponding nematic energy density (2). By analogy, we should also include the relative layer compression, with a third phenomenological constant D_0. Writing this in the specific frame aligned with the layer normal $\|\boldsymbol{z}$ and explicitly presenting all strains, we have

$$F_{int} = \frac{1}{2}D_0\left(\varepsilon_{zz} - \frac{\partial u}{\partial z}\right)^2 + \frac{1}{2}D_1\left[\left(\mathsf{v}^a_{zx} - \frac{\partial u}{\partial x}\right)^2 + \left(\mathsf{v}^a_{zy} - \frac{\partial u}{\partial y}\right)^2\right] - \frac{1}{2}D_2\left[\varepsilon_{zx}\left(\mathsf{v}^a_{zx} - \frac{\partial u}{\partial x}\right) + \varepsilon_{zy}\left(\mathsf{v}^a_{zy} - \frac{\partial u}{\partial y}\right)\right]. \tag{8}$$

The third possible type of layer–network coupling is the penalty on relative translations along $\boldsymbol{z}$ (layer normal), with a contribution to the local free-energy density $\sim\Lambda(u - v_z)^2$ [42]; see figure 4(a). This energy is associated with a barrier that a network cross-link should experience if its displacement $\boldsymbol{v}(\boldsymbol{r})$ attempts to carry it through the smectic layer. The result of such coupling would be the rigid locking of uniform layer rotations and compressions $\nabla_k u$ with the corresponding uniform component of strain, v_{kz}, of the rubbery network. The 'mass' provided by the relative-translation coupling also leads to the suppression of thermal fluctuations and the establishing of a long-range one-dimensional order of layers [43]. A precision x-ray study of the scattering from smectic layers (the technique used with some success to analyse the Landau–Peierls layer fluctuation spectrum in liquid smectic-A) has indeed indicated a Bragg-like scattering intensity $I(q)$ [44]. On the other hand, randomly distributed network cross-links would present sources of quenched disorder for the layer displacement field $u(\boldsymbol{r})$ (see [45] for details), resulting in the equilibrium frustration of layer structure and affecting the properties of phase transitions between nematic and smectic states. An indication of this increased quenched disorder has been observed in another x-ray study of aligned monodomain smectic elastomers [46]. Clearly, the issues of equilibrium order and alignment in smectic networks are far from being resolved. There is obviously an attractive parallel with nematic networks where the depression of thermal fluctuations (and the corresponding increase in local order) is competing with the macroscopic quenched disorder introduced by random cross-links. For instance, many features of the polydomain–monodomain transition have been found in a smectic-A elastomer [47]. However, at times it might be difficult to unambiguously distinguish between the nematic and smectic-A orders in elastomer samples.

Unlike the case for nematic elastomers, up to now there has been no adequate molecular-statistical theory of lamellar networks. All one can say within the continuum phenomenological approach is that the order of magnitude of elastic moduli in a rubbery network has to be $\mu \sim n_c k_B T$. However, this characteristically entropic rubber-elastic response should only be related to locally two-dimensional deformations in the plane of smectic layers. Because the polymer chains are not free to diffuse through the barriers presented by layers, the response to the deformation along the layer normal $\boldsymbol{n}$ ($\|\boldsymbol{z}$ here) should be enthalpic, with the modulus μ_0 large, comparable to the smectic-layer compression constant B; cf. equation (2). Also, remembering our discussion of soft elasticity when the nematic director is completely free to relax, we should expect the effective shear modulus $\tilde{\mu}_2 \to 0$. In smectic elastomers, the

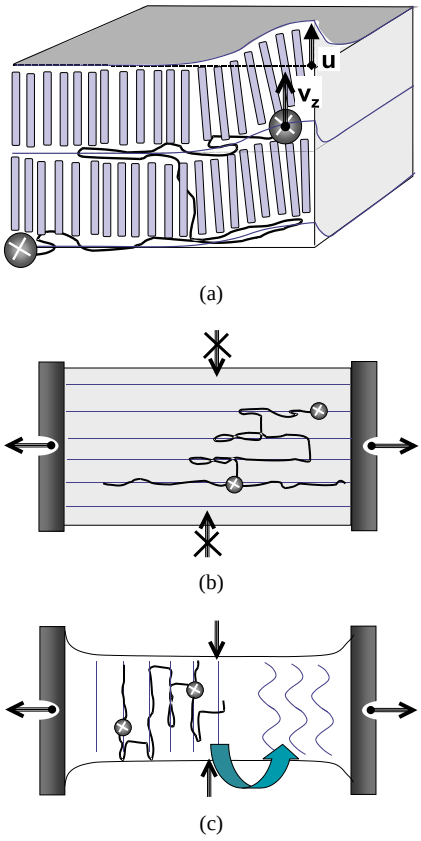

Figure 4. Deformations in smectic elastomers. (a) A schematic representation of layers and the polymer backbone between two cross-links. The chain (shown as a thick line) performs a random walk in the layer plane, but jumps rapidly between layers, forming fully extended strands (layer-forming mesogenic groups are, of course, attached to the backbone which is not shown in the drawing to preserve readability). The deformation of layers $u(\boldsymbol{r})$ is only measured along the undistorted layer normal; the drawing illustrates the relative-translation coupling $\sim(u - v_z)^2$. (b) Stretching the monodomain smectic elastomer in the layer plane preserves the layer integrity but does not allow the transverse contraction (necking). A selected network strand between two cross-links is shown again to illustrate the 2D random-walk property. (c) Stretching along the layer normal causes a strong elastic resistance and results in layer instabilities, initially—Helfrich–Hurault-type undulations.

director cannot completely relieve both network and layer strain. So we could expect the renormalized constant $\tilde{\mu}_2$ to be small but non-zero, proportional to the degree of smectic order, measured by the order parameter amplitude $|\psi|$, at least near the nematic–smectic transition.

Experimental observations of deformations and ordering in smectic elastomers seem to support the idea of two-dimensional entropic rubber elasticity combined with a rigid response along the layer normal from the chain segments constrained between the layers. The strong effect of network shears of the uniform layer rotation has been reported [48] and used to produce aligned monodomain smectic rubbers. Extension in the plane of the layers (figure 4(b)) is resisted by the low elastic modulus $\sim\mu$, but the transverse contraction which is usual for incompressible rubbers does not take place [22]. The layered network can be stretched by a large amount, still preserving its layer integrity and alignment (but, of course, the sample strip has to become thinner if one is to observe the incompressibility constraint). In contrast, the

extension along the layer normal is resisted by a very high modulus, several orders of magnitude greater than μ. The transverse sample contraction and necking is very pronounced [22]. In fact, the uniform layer system cannot be sustained for such deformation geometry, and highly scattering layer undulation textures result [49].

Another interesting development in this area was the preparation and study of physical properties of free-standing thin films of smectic elastomer. In this case a slightly more complex system was used, probably in view of possible electromechanical applications. The ferroelectric smectic-C* polymer has been stretched on a frame into a well-aligned film only several layers thick and then cross-linked by UV radiation [50]. The elastic thin film was then studied by optical and atomic-force microscopy techniques [51], in its natural state and on stretching, with varying cross-linking type and density to examine its mechanical properties and with changing temperature to explore the phase transitions. One particularly unusual result of that work was the effect of increasing surface roughness on stretching an initially smooth film with layers perfectly aligned parallel to its surface. As a possible explanation, one might imagine a deformation-induced effect of local rotation of rod-like mesogenic cross-links, generating an effective polydomain texture in the smectic tilt angle and, thus, the local film thickness, $\langle[h(r) - h(0)]^2\rangle \simeq r/\xi$, similar to that described in section 4.

6. Dynamics and relaxation

The research into dynamical properties and relaxation in LCE has begun only recently. Traditional experimental techniques for studying the complex modulus (frequently called in this context $G(\omega) = G'+\mathrm{i}G''$) include that based on an oscillating dynamic–mechanical (DMA) rheometer, as was used in [52], which examined the frequency range from 10^{-2} to 10^4 Hz as a function of temperature. The authors of [52] observed a marked increase in resistance near and after the nematic–smectic-A transition. However, no particular difference in rheological properties between the nematic and isotropic phases has been seen, and the time–temperature superposition well known for ordinary polymers and rubbers was found to be valid. This is surprising, if we recall the distinctly non-linear elastic behaviour, as shown, for instance, in figure 2(c), and the effect of soft elasticity.

More recent work leads to the question of whether a frequency as low as 10^{-2} Hz is, in fact, low enough for one to observe the effects specific to LCE. The study of stress relaxation [23] in main-chain LCE with a possibly smectic-A order, during the polydomain–monodomain transition, has shown a very slow equilibration of stress after a small strain increment. Within the region examined of up to 6000 s, the relaxation has been fitted to a stretched-exponential form $\sim \exp(-t/\tau)^{0.4}$. Such a type of relaxation is characteristic of many other systems with random glass-like order (or rather disorder) and indicates a broad distribution of relaxation times. Somewhat in contrast to that work, another study of long-time (up to 10^6 s) stress relaxation under very similar conditions (although for a side-chain LCE) [53] has reported that after a characteristic crossover time $t^* \sim 3000$ s, the response is following a much slower, inverse-logarithmic law: $\sigma(t) \sim [1 + \ln(t/t^*)]^{-1}$. An associated theoretical model has been able to relate the critical self-retardation to the random-disorder properties of liquid-crystalline order in the elastic network. The model provides a rate constant vanishing with an essential singularity when the equilibrium is approached, due to the cooperative mechanical barriers to each domain's rotation. The resulting kinetic equation for stress relaxation, having the form $\dot{\sigma} = -m\mathrm{e}^{-u/\sigma}\sigma^3$, gives a solution which at short times resembles the power law $t^{-1/2}$ and at long times can be approximately interpolated as an inverse-logarithmic function, with the crossover time $t^* = (mu^2)^{-1}$. Both regimes correspond well to experimental results [53]. This type of self-retarding behaviour could be universal across randomly disordered systems

where, as in nematic elastomers, the relevant order parameter is coupled to the elastic modes: the mechanical compatibility requires cooperativity of elastic barriers.

At present, the question of relaxation dynamics and kinetic effects in LCE is far from being understood. The pilot research has shown that here, as in their static properties, LCE show many unusual effects. There are new experimental techniques available to examine dynamic processes on all scales, from individual monomers to macroscopic regions of correlated director orientation, which should provide much-needed experimental information. An example of such a multi-scale approach is the recent *in vivo* FTIR study of motion and relaxation of individual mesogenic groups when a LCE sample was macroscopically deformed [54]. The interest in the dynamic properties of anisotropic rubbers and gels has been further promoted by the recently proposed concept of an artificial muscle [55], where the mechanical work is done by an elastomer cycling through its nematic transition (driven by the variation of temperature or chemical composition) and accordingly changing its equilibrium shape, λ_m in figures 1(a) and 1(b).

7. Piezoelectricity and electric field effects

The piezoelectric effect and non-linear optical properties of elastomers with a chiral smectic-C* order (the ferroelectric liquid-crystalline elastomers, FLCE) have been studied with some intensity for several years now. After permanently monodomain (fixed by cross-linking) free-standing samples of FLCE were prepared by the Finkelmann and Zentel groups [50, 56], several useful experiments targeting various electromechanical and electro-optical properties—in particular, the piezoelectricity and the non-linear optical response—have been reported in recent years [57–61]. Clearly, the prospect of important applications will continue to drive this work. In this short review we will concentrate on the analogous effect in chiral nematic LCE which do not possess a spontaneous polarization.

With the much higher symmetry of nematic elastomers (the point group D_∞ in a chiral material, in contrast to C_2, plus the translational effect of layers, in ferroelectric smectic-C*), there is a real possibility of identifying the microscopic origins of piezoelectricity in amorphous polymers or indeed elastomers, if one aims to have an equilibrium effect in a stress-resistant material. The piezoelectric effect in a uniform chiral nematic LCE has been described phenomenologically [62] and, very recently, by a fully non-linear microscopic theory [63]. All experimental research so far has concentrated on the helically twisted cholesteric elastomers [24, 64, 65]. However, the cholesteric texture under the required shear deformation [66] (figure 5(a)) will produce highly non-uniform distortions giving rise to the well-understood

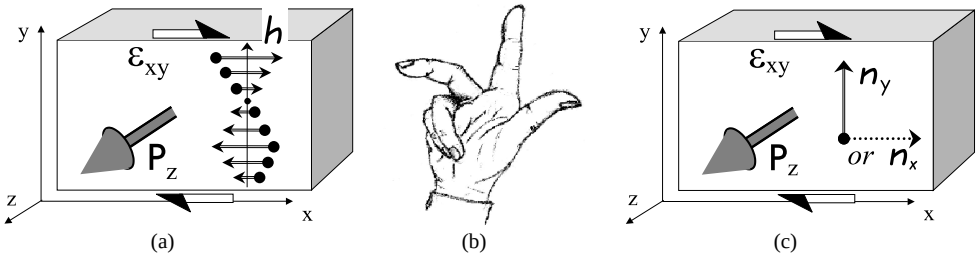

Figure 5. Piezoelectric effects in LCE. (a) Polarization induced by the shear applied to helically twisted textures (the flexoelectric effect). (b) A schematic illustration of the chiral geometry that produces a polarization along z due to the shear and anisotropy axis in the x–y plane. (c) Polarization induced by shearing a uniformly aligned chiral nematic, with the director along either the x-axis or the y-axis (the true piezoelectric effect $\boldsymbol{P} = \gamma[\boldsymbol{n} \times (\underline{\underline{\varepsilon}} \cdot \boldsymbol{n})]$).

flexoelectric effect and masking the possible chiral piezoelectricity.

The uniform linear piezoelectricity, i.e. the polarization induced by a uniform strain—see figure 5(c) (with the small deformation $\varepsilon = \lambda - 1$), is unknown in completely amorphous polymers and rubbers. Even the famous PVDF polymer-based piezoelectric has a response due to crystalline regions affected by deformation. The molecular theory [63] has examined the effect of chirality in the molecular structure of chain monomers and the bias in their short-axis alignment when the chains are stretched at an angle to the average nematic director $\boldsymbol{n}$. If the monomers possess a transverse dipole moment, this bias leads to macroscopic polarization:

$$\boldsymbol{P} \simeq -\frac{1}{2}(n_c\Delta)\underline{\underline{\epsilon}} : (\underline{\underline{\lambda}}^{\mathrm{T}} \cdot \underline{\underline{\ell}}_{\theta}^{-1} \cdot \underline{\underline{\lambda}} \cdot \underline{\underline{\ell}}_{0}). \tag{9}$$

This expression involves the full Cauchy strain tensor $\underline{\underline{\lambda}}$ and, therefore, can describe large deformations of a chiral nematic rubber. When shear deformations are small, the linear approximation of (9) gives, for a symmetric shear,

$$\boldsymbol{P} \simeq \gamma[\boldsymbol{n} \times (\underline{\underline{\varepsilon}} \cdot \boldsymbol{n})]$$

with the linear coefficient

$$\gamma = \partial P/\partial\varepsilon \approx -\frac{1}{2}n_c\Delta(\ell_{\parallel}^2 - \ell_{\perp}^2)/\ell_{\parallel}\ell_{\perp}.$$

Here n_c is the number of network strands per unit volume (the cross-linking density) and the parameter Δ is the measure of monomer chirality with the transverse dipole moment. Piezoelectricity in amorphous rubbers is interesting not only from the point of view of the fundamental physics of chiral random walks and symmetry breaking. On the practical side, due to the rubber modulus being much lower than that for ordinary solid piezoelectrics (typically $\mu \sim 10^5$ J m^{-3}), the relevant coefficient $d = \partial P/\partial\sigma = \gamma/\mu$ is much higher than the corresponding response to stress in, for instance, quartz or PVDF. The corresponding low mechanical impedance should make the piezoelectric rubber attractive for many energy-transducing applications.

Apart from the piezoelectricity, molecular chirality of polymer chains cross-linked into the elastic network presents many fundamental challenges on its own. In linear elasticity, the chirality of the medium does not have any effect on the mechanical response. However, in elastomers and gels the regime of high deformations and non-linear stress–strain relations is readily accessible; liquid-crystalline elastomers are even more characteristic in this way, due to their soft elasticity. Chiral properties of polymers should then show themselves not only in the optical activity, but also, more curiously, in mechanical properties. There has been very little research on this subject, apart form a very interesting study showing the effect of chiral imprinting [67, 68], when the network of non-chiral polymers is cross-linked in the presence of a chiral solvent and then the solvent is removed from the system completely. After this, no molecularly chiral object is left, but the elastomer shows distinctly chiral macroscopic properties, presumably because a specific topology has been imprinted in the cross-link distribution.

8. A look to the future

This review examines the most recent and relevant findings about a new class of materials—liquid-crystalline elastomers and gels. Nematic rubbers have already proved themselves an unusual and exciting system, with a number of unique optical and mechanical properties—indeed a real example of the Cosserat media with couple-stress elasticity. Polymer networks with a smectic order are an equally provocative system, promising new physical properties.

The basic molecular theory of nematic rubber appears to be exceptionally simple in its foundation and does not involve any model parameters apart from the backbone polymer chain anisotropy $\ell_\parallel/\ell_\perp$, which can be independently measured. This represents a great advantage over the situation for many other soft condensed matter systems requiring complicated, sometimes ambiguous theoretical approaches. Of course, for many real situations and materials one finds a need to look deeper into the microscopic properties; an example of this is provided by the 'semi-softness' of nematic networks. Most of these systems are characterized by non-uniform deformations: even in the simplest experimental set-up a large portion of the sample near the clamps is subjected to non-uniform strains and, therefore, responds with a non-uniform director field.

Looking to the future, many challenging and fundamental problems in this field are still outstanding. Smectic and lamellar elastomers and gels have to be studied in much greater detail, theoretically and experimentally, to underpin their dramatically anisotropic and non-linear mechanical properties combining a two-dimensional rubber-elastic response and solid-like properties in the third direction. The field of relaxation and dynamics in rubbery networks, although not young by any means, is still not offering an unambiguous physical picture of stress relaxation. Adding the liquid-crystalline order, we find an additional (director) field undergoing its own relaxation process and coupled to that of an elastic network. In the particular case of polydomain (i.e. randomly disordered in equilibrium) elastomers, we can identify a hierarchical sequence of physical processes in the underlying network (above its T_g) and the superimposed glass-like nematic order. This leads to a particularly slow relaxation, but much remains to be done to understand the physics of such complex systems.

The general problem of dynamic mechanical properties, rheology and relaxation in Cosserat-like incompressible solids, also characterized by the effect of soft elasticity, brings to mind a number of possible applications. An example would be the selective attenuation of certain acoustic waves, with polarization and propagation direction satisfying the condition for softness, essentially leading to an acoustic filtering system. Another example of application of soft elasticity, also related to the problem of relaxation, is the damping of shear vibrations in an engineering component when its surface is covered by a layer of nematic or smectic rubber, particularly aligned to allow the director rotation and softness.

Other very important area of applications is based on polarizational properties of materials with chirality. Most non-linear optical applications (which have a great technological potential) deal with elastomers in the ferroelectric smectic-C* phase. The low symmetry (in particular, chirality) and large spontaneous polarization of C* smectics have a strong effect on the underlying elastic network, and vice versa. This also harks back to the general problem of mechanical properties of smectic rubbers and gels. In conclusion, after the initial period of exploration and material synthesis, liquid-crystalline elastomers, in all their variety, now present themselves as an exciting area for both fundamental research and for technology.

Acknowledgments

I wish to thank M Warner, P D Olmsted, S M Clarke, H Finkelmann and many others, for fruitful and enjoyable collaboration and many stimulating discussions on this subject.

References

[1] de Gennes P G 1975 *C. R. Acad. Sci.* B **281** 101
[2] Finkelmann H, Koch H J and Rehage G 1981 *Macromol. Rapid Commun.* **2** 317

[3] Gleim W and Finkelmann H 1989 *Side-Chain Liquid Crystal Polymers* ed C B McArdle (Glasgow: Blackie) p 287
[4] Barclay G G and Ober C K 1993 *Prog. Polym. Sci.* **18** 899
[5] Warner M and Terentjev E M 1996 *Prog. Polym. Sci.* **21** 853
[6] Brand H R and Finkelmann H 1998 *Handbook of Liquid Crystals* vol 3, ed D Demus *et al* (New York: Wiley–VCH) ch V
[7] Zentel R and Reckert G 1986 *Macromol. Chem.* **187** 1915
[8] Legge C H, Davis F J and Mitchell G R 1991 *J. Physique* II **1** 1253
[9] Zubarev E R, Talroze R V, Yuranova T I, Vasilets V N and Plate N A 1996 *Macromol. Rapid Commun.* **17** 43
[10] Küpfer J and Finkelmann H 1991 *Macromol. Rapid Commun.* **12** 717
[11] Kundler I and Finkelmann H 1998 *Macromol. Chem. Phys.* **199** 677
[12] Brehmer M, Zentel R, Wagenblast G, Siemensmeyer K 1994 *Macromol. Chem. Phys.* **195** 849
[13] Zubarev E R, Yuranova T I, Talroze R V, Plate N A and Finkelmann H 1998 *Macromolecules* **31** 3566
[14] Carfagna C, Amendola E and Giamberini M 1997 *Prog. Polym. Sci* **22** 1607
[15] Cifferi A and Ward I M (ed) 1979 *Ultra High Modulus Polymers* (London: Applied Science)
[16] Zhao W Y, Kloszkowski A, Mark J E, Erman B and Bahar I 1996 *Macromolecules* **29** 2805
[17] Ortiz C, Kim R, Rodighiero E, Ober C K and Kramer E J 1998 *Macromolecules* **31** 4074
[18] Shiota A and Ober C K 1998 *J. Polym. Sci., Polym. Phys.* **36** 31
[19] Bergmann G H F, Finkelmann H, Percec V and Zhao M Y 1997 *Macromol. Rapid Commun.* **18** 353
[20] Fischer P and Finkelmann H 1998 *Prog. Colloid Polym. Sci.* **111** 127
[21] Kundler I and Finkelmann H 1995 *Macromol. Rapid Commun.* **16** 679
[22] Nishikawa E and Finkelmann H 1997 *Macromol. Chem. Phys.* **198** 2531
[23] Ortiz C, Ober C K and Kramer E J 1998 *Polymer* **39** 3713
[24] Chang C-C, Chien L-C and Meyer R B 1997 *Phys. Rev.* E **55** 534
[25] Chang C-C, Chien L-C and Meyer R B 1997 *Phys. Rev.* E **56** 595
[26] de Gennes P G 1980 *Liquid Crystals of One and Two-Dimensional Order* ed W Helfrich and G Heppke (Berlin: Springer) p 231
[27] Olmsted P D 1994 *J. Physique* II **4** 2215
[28] Bladon P, Terentjev E M and Warner M 1994 *J. Physique* II **4** 75
[29] Mitchell G R, Davis F J and Guo W 1993 *Phys. Rev. Lett.* **71** 2947
[30] Talroze R V, Zubarev E R, Kuptsov S A, Merekalov A S, Yuranova T I, Plate N A and Finkelmann H 1999 *Reactive and Functional Polymers* (Amsterdam: Elsevier) at press
[31] Roberts P M S, Mitchell G R and Davis F J 1997 *J. Physique* II **7** 1337
[32] Verwey G C, Warner M and Terentjev E M 1996 *J. Physique* II **6** 1273
[33] Warner M, Bladon P and Terentjev E M 1994 *J. Physique* II **4** 91
[34] Verwey G C and Warner M 1997 *Macromolecules* **30** 4189
Verwey G C and Warner M 1997 *Macromolecules* **30** 4196
[35] Terentjev E M 1997 *Macromol. Symp.* **117** 79
[36] Dotsenko V S 1994 *Theory of Spin Glasses and Neural Networks* (Singapore: World Scientific)
[37] Ogielski A T and Huse D A 1986 *Phys. Rev. Lett.* **56** 1298
[38] Godrèche C, Bouchaud J P and Mezard M 1995 *J. Phys. A: Math. Gen.* **28** L603
[39] Clarke S M, Nishikawa E, Finkelmann H and Terentjev E M 1997 *Macromol. Chem. Phys.* **198** 3485
[40] Fridrikh S V and Terentjev E M 1997 *Phys. Rev. Lett.* **79** 4661
[41] Clarke S M, Terentjev E M, Kundler I and Finkelmann H 1998 *Macromolecules* **31** 4862
[42] Lubensky T C, Terentjev E M and Warner M 1994 *J. Physique* II **4** 1457
[43] Terentjev E M, Warner M and Lubensky T C 1995 *Europhys. Lett.* **30** 343
[44] Wong G C L, de Jeu W H, Shao H, Liang K S and Zentel R 1997 *Nature* **389** 576
[45] Olmsted P D and Terentjev E M 1996 *Phys. Rev.* E **53** 2444
[46] Nishikawa E and Finkelmann H 1998 *Macromol. Rapid Commun.* **19** 181
[47] Ortiz C, Wagner M, Bhargava N, Ober C K and Kramer E J 1998 *Macromolecules* **31** 8531
[48] Benne I, Semmler K and Finkelmann H 1995 *Macromolecules* **28** 1854
[49] Weilepp J and Brand H R 1998 *Macromol. Theory Simul.* **7** 91
[50] Gebhard E and Zentel R 1998 *Macromol Rapid Commun.* **19** 341
[51] Brodowsky H M, Boehnke U C, Kremer F, Gebhard E and Zentel R 1999 *Langmuir* **15** 274
[52] Gallani J L, Hilliou L, Martinoty P, Doublet F and Mauzac M 1996 *J. Physique* II **6** 443
[53] Clarke S M and Terentjev E M 1998 *Phys. Rev. Lett.* **81** 4436
[54] Shilov S V, Skupin H, Kremer F, Wittig T and Zentel R 1997 *Phys. Rev. Lett.* **79** 1686
[55] Hebert M, Kant R and de Gennes P G 1997 *J. Physique* II **7** 909

[56] Finkelmann H, Benne I and Semmler K 1995 *Macromol. Symp.* **96** 169
[57] Brehmer M, Zentel R, Giesselmann F, Germer R and Zugemaier P 1996 *Liq. Cryst.* **21** 589
[58] Brehmer M and Zentel R 1997 *Macromol. Symp.* **117** 53
[59] Eckert T, Finkelmann H, Keck M, Lehmann M and Kremer F 1996 *Macromol. Rapid Commun.* **17** 767
[60] Lehmann W, Gattinger P, Keck M, Kremer F, Stein P, Eckert T and Finkelmann H 1998 *Ferroelectrics* **208** 373
[61] Kremer F, Lehmann W, Skupin H, Hartmann L, Stein P and Finkelmann H 1998 *Polym. Adv. Technol.* **9** 672
[62] Terentjev E M 1993 *Europhys. Lett.* **23** 27
[63] Terentjev E M and Warner M 1999 *Eur. Phys. J.* B at press
[64] Meyer W and Finkelmann H 1990 *Macromol. Chem. Rapid Commun.* **11** 599
[65] Valerien S U, Kremer F, Fischer E W, Kapitza H, Zentel R and Poths H 1990 *Macromol. Chem. Rapid Commun.* **11** 593
[66] Pelcovits R A and Meyer R B 1995 *J. Physique* II **5** 877
[67] Tsutsui T and Tanaka R 1981 *Polymer* **22** 117
[68] Hasson C D, Davis F J and Mitchell G R 1998 *Chem. Commun.* **22** 2515